B: Liquids, Chemical and Dynamical Processes in Solution, Spectroscopy in Solution

Ion Correlation and Collective Dynamics in BMIM/BF Based Organic Electrolytes: From Dilute Solutions to the Ionic Liquid Limit

Jesse Gatten McDaniel, and Chang Yun Son

J. Phys. Chem. B, **Just Accepted Manuscript** • DOI: 10.1021/acs.jpcb.8b04886 • Publication Date (Web): 21 Jun 2018

Ion Correlation and Collective Dynamics in $BMIM/BF_4$ Based Organic Electrolytes: From Dilute Solutions to the Ionic Liquid Limit

Jesse G. McDaniel*,† and Chang Yun Son‡

†*School of Chemistry and Biochemistry, Georgia Institute of Technology, Atlanta, Georgia 30332-0400*

‡*Division of Chemistry and Chemical Engineering, California Institute of Technology, Pasadena, California 91125*

E-mail: mcdaniel@gatech.edu

Abstract

Quantifying ion association and collective dynamical processes in organic electrolytes is essential for fundamental property interpretation and optimization for electrochemical applications. The extent of ion correlation depends on both the ion concentration and dielectric strength of the solvent; ions may be largely uncorrelated in sufficiently high dielectric solvents at low concentration, but properties of concentrated electrolytes are dictated by correlated and collective ion processes. In this work, we utilize molecular dynamics simulations to characterize ion association and collective ion dynamics in organic electrolytes composed of binary mixtures of 1-butyl-3-methylimidazolium tetrafluoroborate $[BMIM^+][BF_4^-]$ and 1,2-dichloroethane, acetone, acetonitrile, and water solvents. We illustrate different physical regimes of characteristically distinct ion correlation for the systematic range of electrolyte concentrations and solvent dielectric strengths. Dilute electrolytes composed of low-dielectric solvents exhibit significant counterion correlation in the form of ion-pairing and clustering driven by both weak screening and relatively low solvation energies. This regime is characterized by enhanced ion coordination numbers and near equality of cation and anion diffusion coefficients, despite the significantly different ion sizes. In contrast, ion correlation in highly concentrated electrolytes is dominated by the anti-correlated motion of both like-charge and opposite-charge ions, approaching neat ionic liquid behavior. We show that the cross-over of these correlation regimes is clearly illuminated by quantifying the fractional self and distinct contributions to the net ionic conductivity. For organic electrolytes composed of low-dielectric solvents, we conclude that significant ion correlation exists at all concentrations, but the nature of the correlation changes markedly from the dilute electrolyte to the pure ionic liquid limit.

1 Introduction

Mixtures of room-temperature ionic liquids and organic solvents are increasingly utilized as electrolytes for electrochemical energy storage devices such as supercapacitors and bat-

teries.[1–3] Organic ions and solvents can be chosen to provide much wider electrochemical stability windows than corresponding aqueous electrolytes, which is necessary for higher operating voltages.[2,4,5] Additionally, organic electrolytes present immense potential for tunability, through numerous choices of ion type and concentration, and because of the miscibility of ionic liquids with many different types of organic solvents. It is important to both quantify, and develop a better fundamental understanding of the substantial modulation of electrolyte properties across the full range of ionic concentration and solvent dielectric strength. Notably, electrolytes of practical interest may be well past the dilute regime and/or exhibit relatively weak dielectric screening, so that ion correlation and collective processes may be of primary importance.

Much research has been devoted to the study of pure ionic liquids, and we refer the interested reader to several excellent review articles.[2,6–10] While room-temperature ionic liquids are fascinating in their own right, these are generally not ideal electrolytes because of their high viscosities, which arise from very large cohesive energies; consequently, the ion dynamics are very slow and conductivities are correspondingly low. Diluting ionic liquids with organic solvents significantly lowers the viscosity and enhances ion diffusion rates.[11–14] Additionally, for many organic electrolyte mixtures, the specific conductivity is maximized at relatively low ion concentration ($\sim$ 0.05-0.2 ion mole fraction).[15,16] This interesting behavior is evidently due to a decrease in molar conductivity with increasing ion concentration, which arises from an approximately inverse dependence on the liquid viscosity;[17] note the viscosity increases by over two orders of magnitude going from the organic solvent to ionic liquid limit. Furthermore, dilution affects both ion fluctuations and Debye screening length, and it has been found that electrolytes with relatively low ionic concentration exhibit exceptional performance in electrical double layer supercapacitors.[18,19] Therefore, organic electrolytes spanning low to high ion content are relevant for electrochemical application, and it is important to understand the significant change in properties over this full concentration range.

Electrolyte properties strongly depend on the ionic concentration which dictates the

viscosity and number of charge carriers. At a specific concentration, however, variation in solvent dielectric strength can substantially alter the extent of ion association and correlation.[17] Quantifying ion association constants and ion correlation as a function of both concentration and solvent dielectric strength is thus fundamental for interpretation, but is experimentally challenging. Association constants may be inferred as proportionality prefactors of molar conductivities, assuming an inverse functional dependence on solution viscosity.[17] Such "Walden plots" exhibit intrinsic uncertainty due to the underlying approximations, and have mainly been utilized for qualititive interpretation of organic electrolyte behavior.[12,14,15] Characterization methods such as dielectric relaxation spectroscopy[20–25] and/or optical Kerr effect spectroscopy[26,27] directly probe the collective dielectric response, providing ion pair interaction signatures in the gigahertz (GHz) through terahertz (THz) frequency regime.[23,28] However, interpretation of these spectra is often very challenging, due to the frequency overlap of many different relaxation modes, and thus complementary theoretical modeling is of great benefit.[29–32]

Collective ion processes are expected to be particularly important for electrolytes composed of low dielectric solvents, and indeed molar conductivity generally exhibits a strong dependence on the solvent dielectric strength.[17] Additionally, for concentrated electrolytes (ionic liquids), significant ion correlation is inferred by observed discrepancies between experimental conductivities and conductivities predicted by idealized, Nernst-Einstein relations.[33–35] Such comparisons provide valuable insight, but caution must be exercised if attempting to quantitatively extrapolate ion association constants.[36] In this regard, computational studies are advantageous in their ability to decompose the ionic conductivity and associated correlation functions into self and distinct (correlated) contributions.[36–40] While previous studies have examined ion association and correlation in pure ionic liquids,[35,36,41] similar computational studies of dilute organic electrolytes have mostly focused on acetonitrile-based systems,[19,42–44] and studies of electrolytes consisting of low-dielectric solvents are relatively scarse. Recently, solvation models have been proposed to predict

ion association constants,[45] and combined molecular simulations and quasi-elastic neutron scattering experiments have demonstrated correlation of ion association and ion dynamics with solvent dielectric strength.[46] While numerous studies exist for ionic liquid/water mixtures,[31,47–56] these systems are deserving of separate discussion due to their unique phase behavior, and the properties of lower dielectric electrolytes may differ significantly (*vide infra*).

Computational characterization of organic electrolytes has been partially hindered by the fact that molecular models (force fields) which were either optimized or benchmarked for pure ionic liquids and/or pure organic solvents, may qualitatively fail to describe the full concentration range of ionic liquid/solvent mixtures.[57] These electrolyte systems span the spectrum of low-cohesive energy, dispersion-dominated solvents (dichloroethane) to very high cohesive energy, electrostatically-dominated ionic liquids; thus accurate computational modeling requires force fields with the correct physical balance of dispersion, electrostatic, and polarization interactions. Ion association varies dramatically with concentration and depends on the ion-pair interaction energies, which are not accurately described by non-polarizable force fields as is well-documented within the context of vaporization enthalpy prediction.[58–61] Additionally, so-called "scaled charge" force fields severely underestimate the cohesive energy of ionic liquids, and do not accurately reproduce ion association trends for varying dielectric solvents.[57] To overcome such limitations, in this work we utilize *ab initio*, polarizable force fields, based on symmetry-adapted perturbation theory (SAPT), as developed previously.[57,61,62] These force fields accurately reproduce the balance of van der Waals and electrostatic interactions in both organic solvents and pure ionic liquids,[61,62] and are explicitly polarizable which is an essential requirement for robustly describing ionic liquid/solvent mixing.[57]

In this work, we study the extent of ion pairing and correlation in organic electrolytes, and the subsequent influence on the ion dynamics and conductivity. We focus on binary electrolyte mixtures consisting of 1-butyl-3-methylimidazolium tetrafluoroborate [$BMIM^+$][BF_4^-]

and 1,2-dichloroethane, acetone, acetonitrile, and water solvents over their full concentration range. Using molecular dynamics simulations, we investigate the change in liquid structure, e.g. the ion pair correlation and ion coordination number, from the dilute electrolyte limit to the pure ionic liquid. We then analyze the ion dynamics and conductivities of the electrolytes over this full concentration range. Substantial physical insight is obtained by decomposing both the specific and molar conductivities into their self (diagonal) and distinct (off-diagonal) components, which quantifies both like-ion and counter-ion correlation. With this analysis, we show that ion correlation is distinctly different at dilute and concentrated regimes. At dilute concentrations in low-dielectric solvents, counter-ion pairing is the dominant correlation effect, giving rise to large, negative cation-anion distinct conductivities. As concentration increases to the pure ionic liquid regime, anti-correlated motion between like-charge ions dominates, resulting in negative cation-cation and anion-anion distinct conductivities. An interesting consequence of this ion correlation is that the cation and anion self-diffusion coefficients, which differ by a factor of $\sim$2 at dilute concentration in high dielectric solvents, are approximately identical in electrolytes composed of low dielectric solvents, as well as in the ionic liquid limit. Because our simulations utilize *ab initio* force fields, this work constitutes a first-principles prediction of the organic electrolyte properties, with predicted conductivities in good agreement with prior experimental measurements over the full concentration range.

2 Methods

Molecular dynamics (MD) simulations are conducted for binary [$BMIM^+$][BF_4^-] and 1,2-dichloroethane, acetone, acetonitrile, and water mixtures for nine different ionic concentrations at 300K, 1bar. The nine concentrations are $\sim$ 0.02, 0.05, 0.1, 0.18, 0.23, 0.29, 0.39, 0.52, and 1.0 ion pair mole fraction (χ), which are chosen to approximately span the low-concentration conductivity peaks and illustrate convergence to the bulk ionic liquid limit. We

utilize the *ab initio*, SAPT-FF force field for all simulations, which is described in the previous work of us and others.[57,61,62] For water-based electrolytes, we utilize a hybrid force-field in which the SWM4-NDP model[63] describes all water-water interactions and SAPT-FF describes water-ionic liquid interactions, as discussed previously.[57] The accuracy of SAPT-FF has been benchmarked for the solvents,[62] $[BMIM^+][BF_4^-]$ ionic liquid,[61] and $[BMIM^+][BF_4^-]$ /solvent mixtures,[57] and in this work we additionally demonstrate that predicted ionic conductivities are in excellent agreement with experiment (*vide infra*). The simulation details are analogous to prior work,[57] but here we perform two independent ~ 50 ns simulations for every electrolyte mixture to better quantify the large statistical uncertainty in the total and distinct ionic conductivities (*vide infra*).

MD simulations are conducted utilizing the GPU-accelerated OpenMM software.[64] For efficiency, polarization is modeled using an extended Langrangian scheme,[65] in which Drude-oscillator degrees of freedom are coupled to a low-temperature bath. To ensure equipartiion and counterbalance heat flow from the 300 K modes to low temperature polarization modes, a Langevin thermostat is employed with a 1 ps $^{-1}$ friction coefficient. Such temperature coupling will somewhat perturb the predicted dynamic properties,[66] including diffusion coefficients and conductivities. However this should not significantly alter the qualitative trends found for different solvents and different ionic concentrations, which are the main conclusions of this work. The particle-mesh Ewald (PME) method[67] is used for electrostatics, van der Waals (VDWs) interactions are truncated at 1.4 nm, and a Monte Carlo barostat is employed for pressure coupling. Note that we omit a spherical long-range correction when truncating VDWs interactions, which partially offsets omission of explicit three-body dispersion terms,[62] and is consistent with our previous force-field benchmarks for these systems.[57,61] For the lower ionic concentrations (< 0.2 mole fraction), systems consist of 1000 solvent molecules and 20, 55, 110, and 220 ion pairs. For the higher concentrations, systems consist of 220 ion pairs and 750, 550, 350, 200, and 0 solvent molecules. These system choices provide relatively similar simulation box sizes of $\sim$ 4-6 nm, with slightly smaller systems for

the water-based electrolytes. Initial systems were prepared using the Packmol software,[68] and equilibrated for 10 ns in the NPT ensemble to ensure adequate mixing. Production runs were conducted in the NVT ensemble for 40 ns, and as stated duplicate independent simulations were utilized to estimate uncertainty in the computed conductivities.

We compute probability distribution functions and corresponding coordination numbers for ion pair association in the electrolytes. Because the ionic concentration is not constant in these electrolytes, we focus on the correlation metric[69]

$$\frac{1}{\rho_{ion}}\rho^{(2/N)}(0,\mathbf{r}) = \rho_{ion}g(r) \tag{1}$$

Where g(r) is the ion-ion radial distribution function. While the radial distribution function $g(r)$ is commonly used for interpretation of liquid structure, the fact that it is implicitly normalized by the ionic density can lead to misinterpretation in concentration-dependent studies, and we suggest that it is better to consider the explicit pairwise probability instead. The ion coordination number for electrolyte solutions is then

$$N_{coord} = \int_0^{R_{pair}} 4\pi r^2 \rho_{ion} g(r) dr \tag{2}$$

We have chosen $R_{pair} = 7$ Å corresponding to the minima in the cation-anion correlation functions (*vide infra*). Using a similar distance metric for ion-pair association ($R_{pair} = 7$ Å), the lifetime of an ion-pair,τ_{IP}, is computed as the time at which the survival probability of an ion pair, P(t), decays to 1/e. P(t) is given by the correlation function of an operator h(t) that is unity when a specific ion pair is formed at time t and zero otherwise, as detailed elsewhere.[70]

The conductivity of the electrolyte solutions is given by

$$\sigma_{tot} = \lim_{t\to\infty} \frac{1}{6tVk_BT} \sum_{i,j}^{n} \left\langle (q_i[\mathbf{R}_i(t) - \mathbf{R}_i(0)]) \cdot (q_j[\mathbf{R}_j(t) - \mathbf{R}_j(0)]) \right\rangle \tag{3}$$

where the sum runs over all cations and anions *i, j*, with charges q_i and positions R_i. We will show that it is extremely insightful to decompose the total conductivity into self and distinct terms, by partitioning the sum in Equation 3 into diagonal and off-diagonal contributions, so that[39,40]

$$\sigma_{tot} = \sigma^s_{cat} + \sigma^s_{an} + \sigma^d_{cat} + \sigma^d_{an} + \sigma^d_{cat,an} \tag{4}$$

The cation-self (σ^s_{cat}), anion-self (σ^s_{an}), cation-distinct (σ^d_{cat}), anion-distinct (σ^d_{an}), and cation/anion-distinct ($\sigma^d_{cat,an}$) conductivities are given by

$$\sigma^s_{cat} = \lim_{t\to\infty} \frac{1}{6tVk_BT} \sum_{i}^{cation} \left\langle (q_i[\mathbf{R}_i(t) - \mathbf{R}_i(0)]) \cdot (q_i[\mathbf{R}_i(t) - \mathbf{R}_i(0)]) \right\rangle \tag{5}$$

$$\sigma^s_{an} = \lim_{t\to\infty} \frac{1}{6tVk_BT} \sum_{i}^{anion} \left\langle (q_i[\mathbf{R}_i(t) - \mathbf{R}_i(0)]) \cdot (q_i[\mathbf{R}_i(t) - \mathbf{R}_i(0)]) \right\rangle \tag{6}$$

$$\sigma^d_{cat} = \lim_{t\to\infty} \frac{1}{6tVk_BT} \sum_{i}^{cation} \sum_{j\neq i}^{cation} \left\langle (q_i[\mathbf{R}_i(t) - \mathbf{R}_i(0)]) \cdot (q_j[\mathbf{R}_j(t) - \mathbf{R}_j(0)]) \right\rangle \tag{7}$$

$$\sigma^d_{an} = \lim_{t\to\infty} \frac{1}{6tVk_BT} \sum_{i}^{anion} \sum_{j\neq i}^{anion} \left\langle (q_i[\mathbf{R}_i(t) - \mathbf{R}_i(0)]) \cdot (q_j[\mathbf{R}_j(t) - \mathbf{R}_j(0)]) \right\rangle \tag{8}$$

$$\sigma^d_{cat,an} = \lim_{t\to\infty} \frac{2}{6tVk_BT} \sum_{i}^{cation} \sum_{j}^{anion} \left\langle (q_i[\mathbf{R}_i(t) - \mathbf{R}_i(0)]) \cdot (q_j[\mathbf{R}_j(t) - \mathbf{R}_j(0)]) \right\rangle \tag{9}$$

A standard metric for the extent of ion correlation is the ratio of the total conductivity to that predicted by the Nernst-Einstein equation assuming entirely dissociated, uncorrelated ions,[35,70,71]

$$\sigma^{NE}_{tot} = \sigma^s_{cat} + \sigma^s_{an} = \frac{Nq^2}{Vk_BT}(D_+ + D_-) \tag{10}$$

where D_+, D_- are the cation and anion self-diffusion coefficients, N is the number of ion

pairs, and the notation σ_{tot}^{NE} signifies the Nernst-Einstein approximation.

The total and distinct conductivities from Equations 3 and 7 - 9 are subject to significant statistical uncertainty, an issue which is obscured by the relative ease of calculating the Nernst-Einstein conductivity (Equation 10), the latter benefiting from statistics collected from N independent ions. Indeed the self conductivity terms computed in this work exhibit extremely small statistical uncertainties (*vide infra*). In contrast, the distinct conductivities are collective properties, and require long simulation times for adequate sampling/averaging. We quantify the significant statistical uncertainties in these quantities as follows. Two independent simulations of $\sim$ 40 ns production are conducted for each electrolyte mixture, and we take the difference between computed distinct conductivities from these simulations. Error bars are determined by averaging these differences from simulations at the three nearest ion concentrations. Thus the error for each quantity is determined by six independent simulations, at three different concentrations. For the linear regression required to obtain the conductivities, we choose $\sim$ 1 ns for the elapsed time. Longer elapsed times exhibit highly non-linear behavior, due to poor statistics from ion correlation. We note that the full production trajectories are used for ensemble averaging.

3 Results

The extent of ion correlation in the electrolyte mixtures is quantified from analysis of both structural and dynamical properties. Ion correlation results in ion pairing and clustering within the electrolyte, and leads to deviations of the ionic conductivity from ideal Nernst-Einstein behavior and additionally in the coupling of cation and anion diffusion coefficients. In Figure 1 we show simulation snapshots of [$BMIM^+$][BF_4^-] /dichloroethane and [$BMIM^+$][BF_4^-] /acetonitrile electrolyte mixtures at low ion content (χ_{ion}=0.02). These snapshots qualitatively depict the nature of ion correlation that is the focus of the work. In the dichloroethane-based electrolyte, the ion distribution is clearly not homogeneous, but

rather most ions are paired or clustered with counterions of opposite charge. This emphasizes the qualitative difference between organic electrolytes composed of low-dielectric solvents compared to aqueous electrolytes. For solvents with low dielectric strength ($\epsilon \sim 10$ for dichloroethane), ion screening is significantly reduced, and there is notable ion pairing and correlation. Acetonitrile has intermediate dielectric strength, and in Figure 1 it is evident that the extent of ion pairing is lower than in dichloroethane solvent at similar ion fraction. We quantify how such differences in ion correlation affect ion coordination numbers, diffusion coefficients, and relative self and distinct contributions to the ionic conductivity.

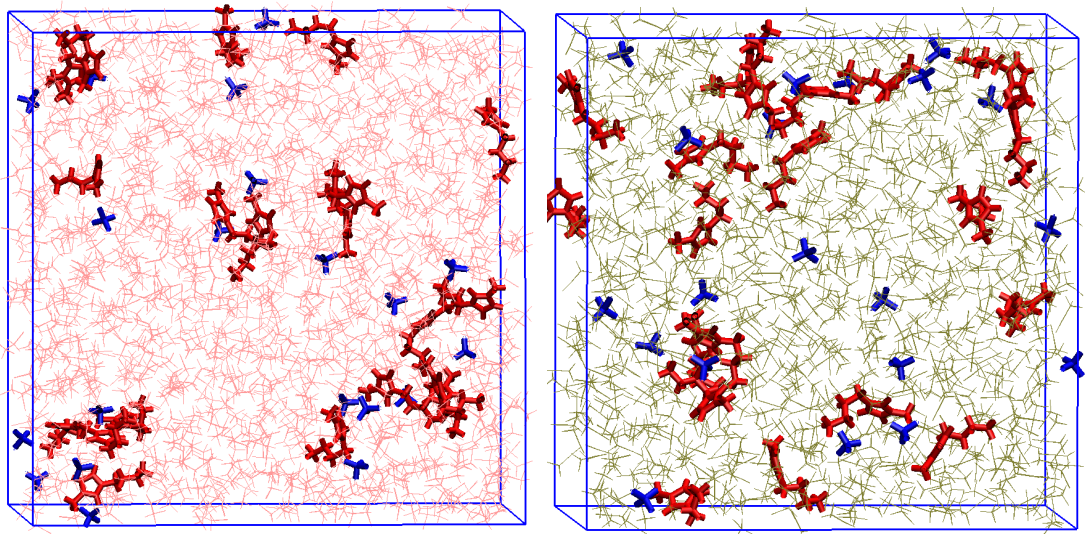

Figure 1: Simulation snapshots of $BMIM^+$and BF_4^-ions in dichloroethane and acetonitrile solvents under dilute conditions (χ_{ion}=0.02). Coloring scheme is $BMIM^+$(red), BF_4^-(blue), dichloroethane (pink), acetonitrile (tan), and the solvent is illustrated with thin lines for clarity.

In Figure 2, we show pairwise probability distributions (Equation 1) for cation/anion coordination in the $[BMIM^+][BF_4^-]$ based electrolytes at different concentrations. As discussed, these distributions are normalized by the ion concentration, so that the spherical integral provides the ion coordination number. We choose the imidazolium ring carbon atoms of $BMIM^+$and the BF_4^-center-of-mass to compute correlation functions, as these ring carbon atoms and $BF_4^-$are the dominant interactions in the neat ionic liquid.[72] As evident in Figure 2, the extent of cation/anion coordination (peak heights) is significantly dependent on

both ion concentration and the solvent dielectric strength; however the shapes of the distribution functions are qualitatively similar for the different electrolytes and the neat ionic liquid (χ=1). All electrolytes show bimodal cation/anion association peaks at $\sim$ 4.0 and 5.7 Å at all concentrations. These peaks correspond to BF_4^-coordination near the three ring carbon atoms of $BMIM^+$, with the two peaks reflecting coordination on both sides of the ring. In dilute electrolytes, this pairwise cation/anion coordination is the only significant ion structure, evidenced by the flatness of the distribution for $r > 7$Å. As the ion concentration increases, secondary ion coordination structure begins to appear corresponding to the emergence of two broad peaks over 7Å $< r <$ 20 Å lengthscale that resemble the structure of neat $[BMIM^+][BF_4^-]$.

The primary solvent effect on the electrolyte liquid structure is manifest in the relative peak heights (coordination number) and onset of ion secondary structure as a function of ion concentration. Lower dielectric solvents promote greater ion association correponding to greater peak intensities for cation/anion correlation, and the onset of ion secondary structure in the electrolyte occurs at lower concentration (Figure 2). For example in dichloroethane electrolytes, the secondary ion structure (peaks between 7 Å$< r <$ 20 Å) emerges at relatively low ion content ($\chi \sim 0.1$), while higher dielectric solvents such as acetonitrile require higher ion concentration ($\chi \sim$ 0.2-0.3) for formation of ion secondary structure. In Figures 3 and 4 we show the corresponding cation/cation and anion/anion pairwise distributions in the electrolytes, from which the ion secondary structure and clustering is more clearly illustrated. At low ion content, most electrolytes show negligible like-ion correlation, except for dichloroethane electrolytes in which there is significant cation/cation (Figure 3) and anion/anion (Figure 4) correlation. This like-ion correlation indicates ion clustering mediated by strong counterion interactions, and is due to the low dielectric screening of the solvent. Unlike the cation/anion correlation (Figure 2), the shape of the cation/cation and anion/anion pairwise correlation is markedly different for the different solvents: Dichloroethane electrolytes are characterized by sharper peaks in the like-ion correlation; acetone and ace-

tonitrile electrolytes exhibit flat distributions at low concentration and broader peaks at higher concentration; and water electrolytes show the broadest like-ion distributions that slowly converge to the neat ionic liquid structure. Interestingly, the cation/cation (Figure 3) and anion/anion (Figure 4) correlations are qualitatively different in structure, indicating the different sizes and solvation of the cations and anions. We note that due to the different sizes of solvent molecules, ion volume fractions can significantly differ at a given mole fraction (χ), and thus comparisons may be best made across same ion volume fraction (*vide infra*).

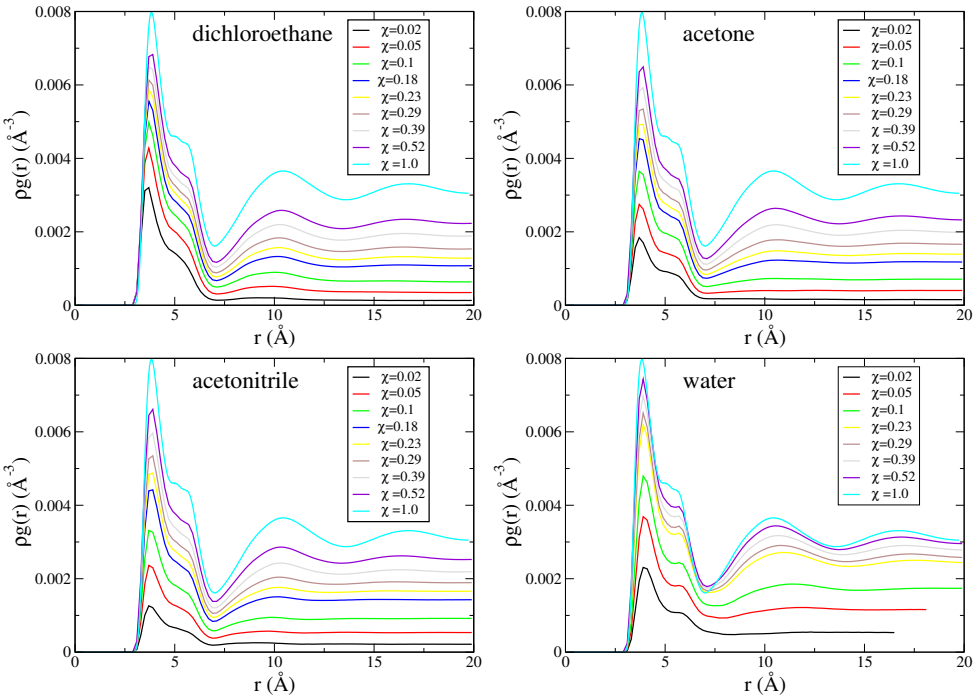

Figure 2: Cation/anion pairwise probability distribution for [BMIM$^+$][BF$_4^-$] / dichloroethane, acetone, acetonitrile, and water mixtures at varying ion mole fraction (χ). RDFs for [BMIM$^+$][BF$_4^-$] /water at low concentrations are computed to shorter range due to smaller box sizes.

From a practical perspective, one of the most important metrics characterizing electrolytes is the ion coordination number, which directly affects the conductivity and other electrical properties. In Figure 5 we plot the cation/anion coordination number (N$_{coord}$) as a function of ion mole fraction (χ_{ions}) for the four different solvents, obtained by integrating the distributions of Figure 2. Interestingly, when plotted as a function of χ_{ions} (Figure

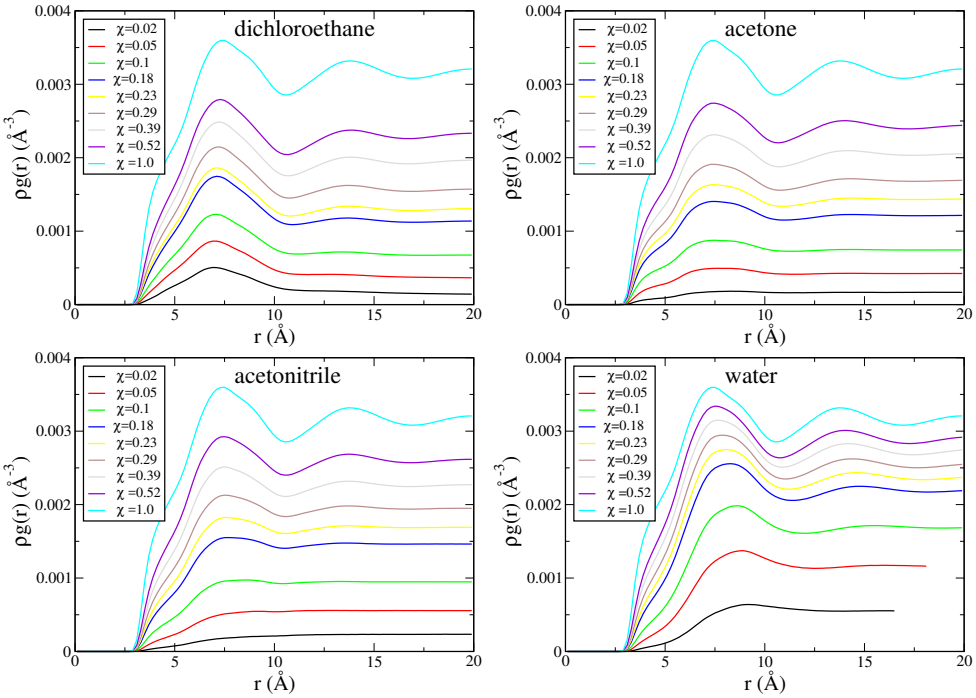

Figure 3: Cation/cation pairwise probability distribution for $[BMIM^+][BF_4^-]$ / dichloroethane, acetone, acetonitrile, and water mixtures at varying ion mole fraction (χ). RDFs for $[BMIM^+][BF_4^-]$ /water at low concentrations are computed to shorter range due to smaller box sizes.

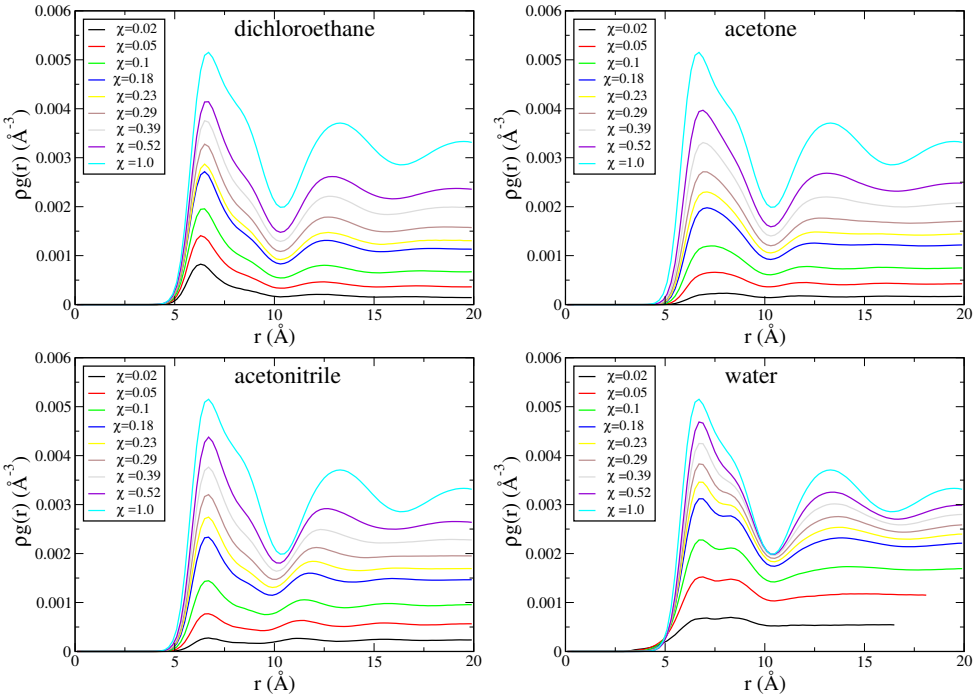

Figure 4: Anion/anion pairwise probability distribution for [BMIM$^+$][BF$_4^-$] / dichloroethane, acetone, acetonitrile, and water mixtures at varying ion mole fraction (χ). RDFs for [BMIM$^+$][BF$_4^-$] /water at low concentrations are computed to shorter range due to smaller box sizes.

5a), there is little evident correlation between coordination number and solvent dielectric strength, and the dependence of N_{coord} on χ_{ions} is highly non-linear. However, it has been previously observed that solvent-dependent trends are much more apparent when analyzed in terms of ionic volume fraction rather than mole fraction.[17] A much clearer physical picture emerges in Figure 5b, in which the same coordination number data is plotted against the volume fraction of ions, Φ_{ions} (calculated assuming ideal mixing). In this plot, the ion coordination number shows more linear convergence to the bulk ionic liquid limit (N_{coord}=5), and there is a clear dependence on solvent dielectric strength with smaller ion coordination numbers for higher dielectric solvents. The higher the solvent dielectric, the more linear the N_{coord} vs Φ trend due to greater screening of ion pairs. Water-based electrolytes exhibit somewhat higher ion coordination number than predicted based solely on dielectric trends, which may be due to the unique hydrogen bond structure of water.

Our analysis of ion coordination in various dielectric solvents results in the following structural picture of organic electrolytes. The energy of association of cation/anion pairs in the gas phase is very large ($>$ 350 kJ/mol for $[BMIM^+][BF_4^-]$), and in absence of a dielectric medium the ions would always be found as ion-pairs or clusters at low concentration.[61] In low dielectric solvents such as dichloroethane, analogous physics leads to significant ion-pairing and clustering at low concentration, evidenced by the counterion correlation (Figure 2), like-ion correlation (Figure 3 and 4), and counterion coordination number (Figure 5). With increasing solvent dielectric (acetonitrile, water) ions are increasingly solvated, with less counterion correlation and negligible secondary ion structuring at low concentrations. The nature of solvent dictates the convergence of electrolyte ion structure to the neat ionic liquid limit, which is best observed through analysis of ion clustering and secondary ion structure revealed in the like-ion correlation functions (Figure 3 and 4). The approximately linear trend in counterion coordination number with volume fraction (Figure 5b) suggests that volume fraction instead of mole fraction should be used to compare electrolyte solutions across different concentrations and solvents.

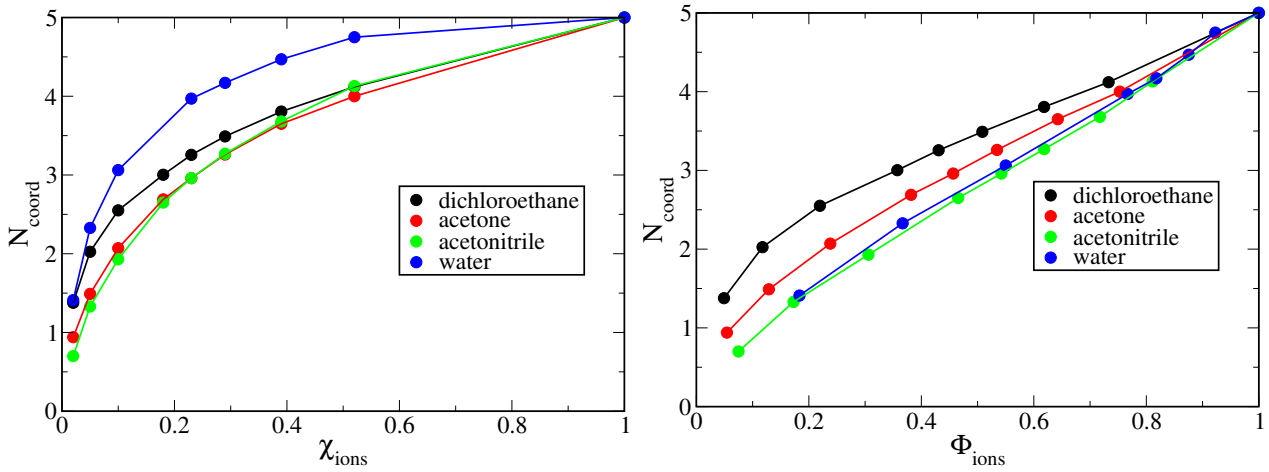

Figure 5: Counterion coordination number (N_{coord}) of [BMIM$^+$][BF$_4^-$] ions in dichloroethane, acetone, acetonitrile, and water solvents as a function of a) ion mole fraction (χ_{ions}) and b) ion volume fraction (Φ_{ions}).

The extent of ion coordination has a very significant effect on the collective ion mobility and resulting conductivity of the electrolyte. As will be discussed, the net conductivity results from highly correlated, collective ion motion that exhibits a complex dependence on ion concentration and solvent dielectric strength. For physical insight, we first compute the ion self-diffusion coefficients as a function of concentration in the different electrolytes. In Figure 6 we show cation (D_{BMIM}) and anion diffusion coefficients (D_{BF_4}) as a function of concentration for the different electrolytes. The most apparent trend is the extreme decrease in diffusion rates with increasing ion concentration, which is due to the 2-3 order of magnitude increase in electrolyte viscosity going from dilute electrolyte ($\eta \sim$ 0.4-1.0 cP) to pure ionic liquid ($\eta \sim$ 100 cP).[60] It is interesting to evaluate the applicability of the Stokes-Einstein relation for the different solvents in the dilute electrolyte limit,

$$D = \frac{k_B T}{6\pi\eta r} \tag{11}$$

which predicts that the diffusion coefficients will be inversely proportional to the solution viscosity and radius of diffusing species. Because the viscosity dependence on concentration

is complex, and significantly varies with solvent,[17] we only discuss the dilute electrolyte limit. The solvent viscosities increase in order acetone < acetonitrile < dichloroethane < water. In the dilute limit, Figure 6 indicates that the solvent viscosities only partially determine the magnitude of D_{BMIM}, D_{BF_4}, and the Stokes-Einstein relation does not entirely capture the variation of ion mobility. Rather, the cation and anion diffusion coefficients are significantly modulated by ion correlation, the extent to which depends strongly on the dielectric strength of the solvent.

An interesting and illuminative property of neat ionic liquids is that diffusion coefficients of cations and anions are often very similar in magnitude, despite significant differences in ion size and shape; for example, in pure $[\mathrm{BMIM}^+][\mathrm{BF}_4^-]$ ionic liquid, cation and anion diffusion coefficients are both $\sim 0.01 * 10^{-5} cm^2/s$.[61] This near equivalence of ion diffusion coefficients hints at the nature of collective ion motion resulting from strong correlation within the ionic liquid. In Figure 6, we see that under dilute conditions in higher dielectric solvents (acetone, acetonitrile, water), there are significant differences between diffusion coefficients of cations and anions, with $D_{BMIM} < D_{BF_4}$ as expected based on ion size. With increasing ion concentration, however, differences between D_{BMIM} and D_{BF_4} become smaller and the cation/anion diffusion becomes nearly indistinguishable in the concentrated electrolyte limit. This clearly indicates a shift in physical diffusion mechanisms, in which the ions no longer diffuse individually at high concentration, but rather ion mobility is determined by collective behavior; this will be discussed in more depth within the context of self and distinct ionic conductivities.

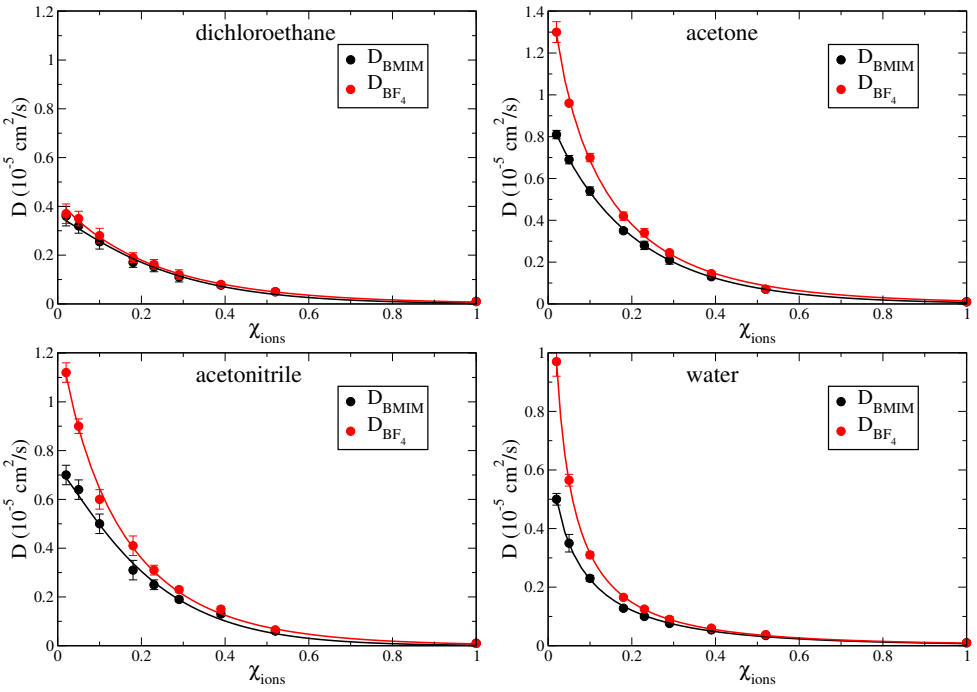

Figure 6: Diffusion coefficients for $BMIM^+$cations and BF_4^-anions as a function of varying ion mole fraction (χ_{ions}) in dichloroethane, acetone, acetonitrile, and water. The curves are stretched exponentials fit to the calculated data (symbols), and are to guide the eye.

Interestingly, the cation and anion diffusion coefficients in dichloroethane-based electrolytes are nearly identical to each other at all concentrations! This is because ions are nearly always paired in dichloroethane due to the relatively low solvent dielectric strength, as qualitatively suggested by the simulation snapshot shown in Figure 1, and confirmed by previously computed ion-pair association free energies.[57] The fact that electrolytes composed of low dielectric solvents consist predominantly of cation/anion pairs and not free ions, even at dilute concentrations, has fundamental implications for physical interpretation. Mean-field theories such as Debye-Huckel and Gouy-Chapman-Stern invoke an ansatz of isolated, independent ions and thus do not accurately capture experimental behavior, an example being the "anomalous" capacitence of organic electrolytes in electrical double-layer capacitors.[18] In addition, an ideal Nernst-Einstein model for conductivity quantitatively fails due to the neglect of important distinct conductivity contributions that result from ion correlation (*vide infra*). We note that the predominance of ion pairs in low dielectric solvents is

reminiscent to the nature of pure ionic liquid vapors. It is now widely accepted that ionic liquid vapors consist predominantly of cation/anion pairs,[61] and thus as the dielectric of the solvent approaches unity, dissolved ions will exist as ion pairs analogous to the ionic liquid vapor regime.

In Figure 7, we plot the same diffusion coefficients, but as a function of ion volume fraction (Φ_{ions}) rather than ion mole fraction. Similar to ion coordination number (Figure 5), trends with solvent dielectric strength are much more apparent when normalized by ion volume fraction. In Figure 7 it is clear that at low ion volume fraction, the deviation between cation and anion diffusion coefficients is larger for higher dielectric solvents. This reflects the extent of ion pairing at low concentration, with greater ion pairing leading to more similar cation/anion diffusion coefficients.

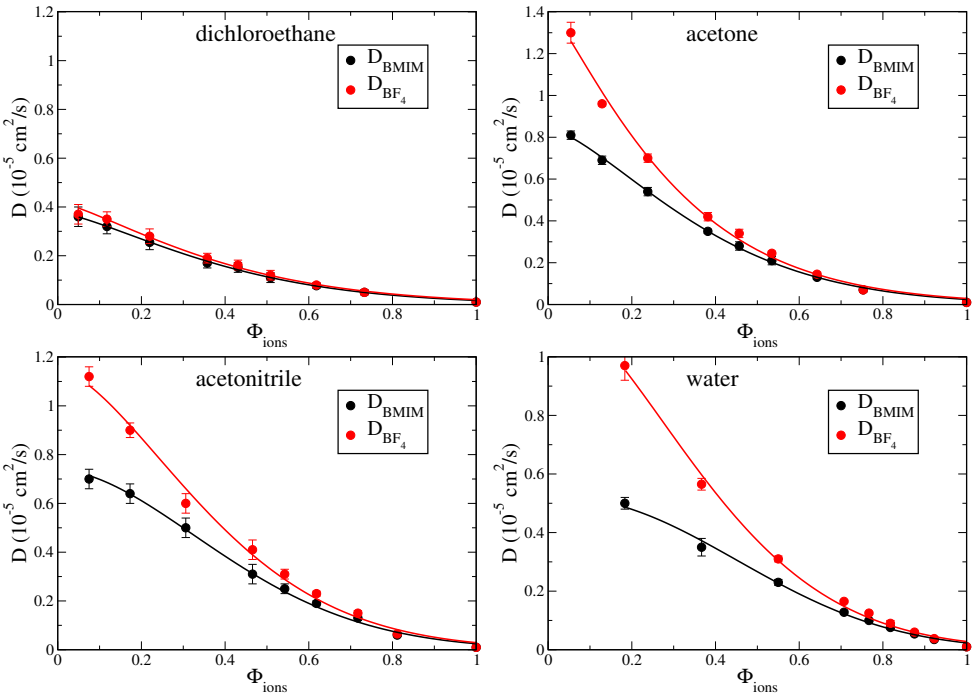

Figure 7: Diffusion coefficients for $BMIM^+$cations and BF_4^-anions as a function of varying ion volume fraction (Φ_{ions}) in dichloroethane, acetone, acetonitrile, and water. The curves are stretched exponentials fit to the calculated data (symbols), and are to guide the eye.

We next discuss the ionic conductivities of the electrolytes; from an experimental standpoint, conductivities constitute the primary information source for determining ion correla-

tion and coordination number in electrolyte mixtures.[12,17] Computed ionic conductivities of the $[BMIM^+][BF_4^-]$ electrolyte mixtures are shown in Figure 8, and are compared to experimentally determined values from Li et al.[17] and Stoppa et al.[12] Our predicted conductivities are in good agreement with experimental values, considering both the statistical uncertainty of the simulations as well as experimental discrepancies. We are not aware of analogous experimental conductivity measurements for the $[BMIM^+][BF_4^-]$ /dichloroethane electrolytes; however, we note that our predicted conductivities agree very well with experimental conductivities for similar electrolytes, consisting of dichloroethane solvent and $EMIM^+/TFSI^-$ionic liquid mixtures.[18] Specific conductivities are characterized by a peak at relatively low ion fraction, which is a result of the exponential decay in molar conductivity multiplied by the linear increase in charge carriers with increasing concentration (*vide infra*). The maximum conductivities vary significantly between electrolytes and occur at dilute ion concentrations, in the range $0.05 < \chi < 0.25$. As we will show, the maximal conductivity value is strongly dependent on both ion self diffusion rates and collective ion diffusion, the former affected by the solvent viscosity and the latter mediated by the solvent dielectric strength. Water and dichloroethane are more viscous than acetone and acetonitrile, and dichloroethane additionally has the lowest dielectric constant of the four solvents, explaining the significantly lower conductivity for $[BMIM^+][BF_4^-]$ /dichloroethane electrolytes. As we discuss next, conductivity trends for the other electrolytes are best explained by decomposing the ionic conductivity into self and distinct contributions.

As suggested by Equations 3 - 9, the total conductivity of the electrolytes results from complex interplay of ion self-diffusion and correlated ionic motion, the balance of which significantly depends on ion concentration and solvent dielectric strength. Employing Equations 5 - 9, we decompose the total electrolyte conductivities (Figure 8) into self and distinct terms, and plot the resulting contributions in Figure 9. This decomposition allows the assessment of both the validity of the Nernst-Einstein approximation (Equation 10), as well as the particular nature of ion correlation leading to any observed deviation. By defini-

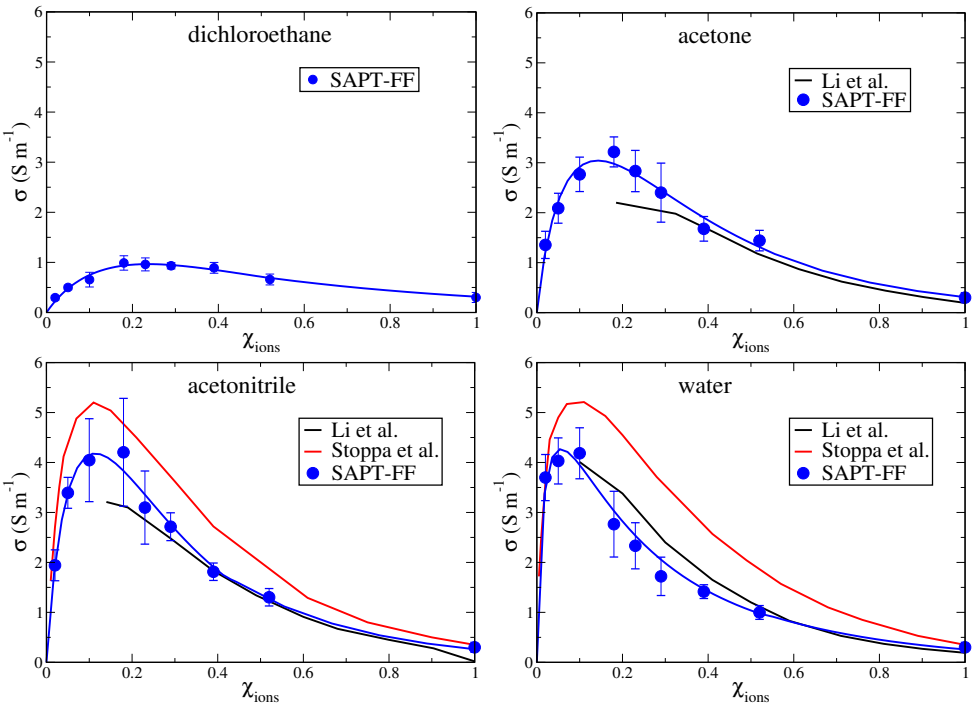

Figure 8: Specific conductivities for $[BMIM^+][BF_4^-]$ / dichloroethane, acetone, acetonitrile, and water electrolytes at varying ion fraction (χ_{ions}). Experimental data is taken from Li et al.[17] and Stoppa et al.[12]

tion, ideal behavior requires σ^d_{cat}=σ^d_{an}=$\sigma^d_{cat,an}$=0, such that ionic motion is uncorrelated, but the Nernst-Einstein relation could also appear accurate through subtle cancellation of these terms. We note that the concentration dependence of specific conductivities is generally fit by the empirical Casteel-Amis equation,[12,73] but in Figures 8 and 9 we have used simpler stretched exponentials with linear prefactors for curve fitting.

In Figure 9, the large differences in ionic conductivity of the different electrolytes are explained in terms of the very different collective ion behavior in these mixtures. There are stark differences in the self and distinct conductivity terms for the electrolytes of low-dielectric solvents (dichloroethane) compared to electrolytes of high-dielectric solvents (acetonitrile, water). The distinct conductivity terms are generally smaller in magnitude in higher dielectric compared to low-dielectric solvents, implying that the ions diffuse more independently when there is greater solvation and screening. Analogous to the ion diffusion coefficients in high-dielectric solvents (Figure 6), the anion-self conductivity term is larger in

magnitude than the cation-self conductivity, indicating the greater mobility of the smaller anions. Note the self terms always contribute positively to the total conductivity, whereas the distinct terms may either raise or lower the total conductivity, depending on the nature of ion correlation. An interesting and important effect in the high-dielectric solvents is that the cation/anion-distinct conductivity term switches sign going from low-concentrated electrolytes (negative) to high-concentration electrolytes (positive). This indicates a shift in the nature of ion correlation, and will be discussed in more depth within the context of Figure 11 (*vide infra*).

For the lower dielectric, dichloroethane electrolytes, the cation/anion-distinct conductivity term dramatically lowers the total ionic conductivity. This is a larger contribution than any other self or distinct term, and indicates the very prominent counterion pairing in these mixtures (positive correlation in Equation 9). The ions exist mostly as ion pairs or clusters, and when moving together there is no net transport of charge, i.e. the charge-neutral pairs do not contribute to the net conductivity. A result is that the cation-self and anion-self contributions to the conductivity are nearly equal, analogous to the equality of the ion diffusion coefficients (Figure 6), but are largely counterbalanced by the cation/anion-distinct term. Interestingly, in these dichloroethane electrolytes, the cation-distinct and anion-distinct conductivity contributions are positive at low ion concentration, in contrast to the higher dielectric electrolytes for which they are negative. Positive contribution of cation-distinct and anion-distinct conductivities should be viewed as the exception to expected behavior; one intuits that diffusion of like-charge ions is anti-correlated, reducing net conductivity. However, like-ion correlation can be facilitated through the mediating counterions, when the ions are paired. The physical picture for conductivity of dichloroethane electrolytes (Figure 9) is that motion of a cation or anion drags along its associated counter-ion, which further pulls along ions of the same charge as the initial ion.

We note that certain care must be taken when interpreting the distinct conductivities, as these quantities are not fully independent in concentrated ionic solutions, but constrained

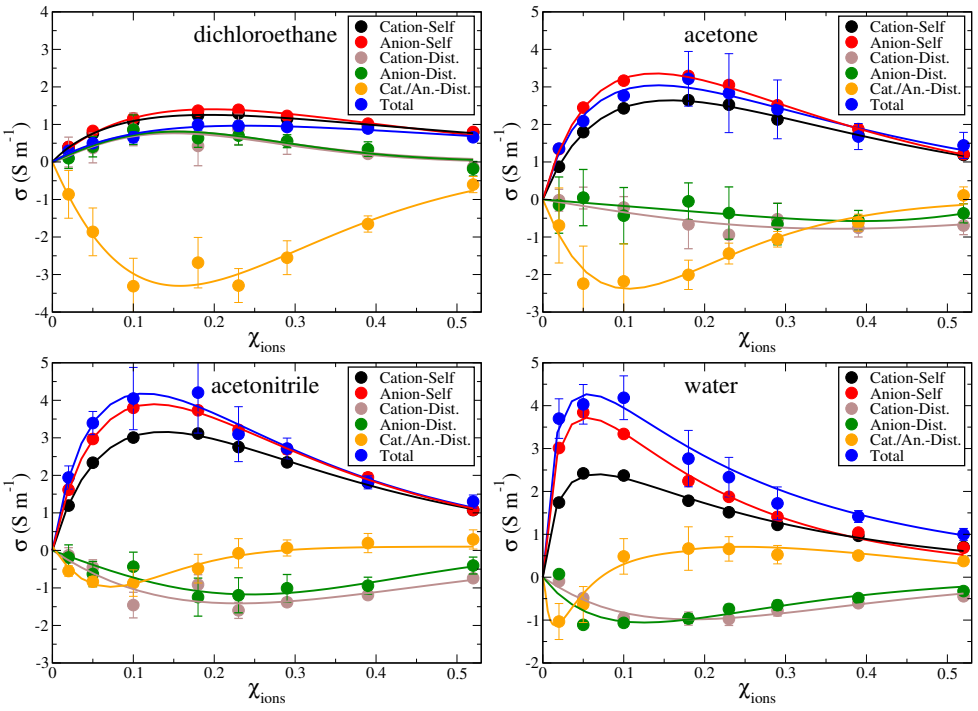

Figure 9: Self and distinct specific conductivities for $[BMIM^+][BF_4^-]$ / dichloroethane, acetone, acetonitrile, and water electrolytes at varying ion fraction (χ_{ions}), as defined by Equations 3 - 9.

by conditions of momentum conservation. A consequence is that distinct conductivities are reference-frame dependent;[37,39] we have considered the system center-of-mass reference frame for simplicity, and have removed all (numerical) center-of-mass motion. At higher ion concentrations, and indeed in the neat ionic liquid limit, the momentum conservation constraint means that the initial velocities of ions are not independent but are correlated, which affects ion motion and the distinct conductivities.[37] For a pure ionic liquid, conservation of center-of-mass momentum implies a direct relation between the three quantities σ^s_{cat}, σ^d_{cat}, $\sigma^d_{cat,an}$ and additionally the three quantities σ^s_{an}, σ^d_{an}, $\sigma^d_{cat,an}$, which has consequences for the applicability of the Nernst-Einstein approximation.[39] For a dilute electrolyte, such rigorous conservation relations are formally relaxed, as solvent momentum can offset ion momentum; however, we do not further discuss this technicality as our focus is on physical interpretation of ion concentration and dielectric effects.

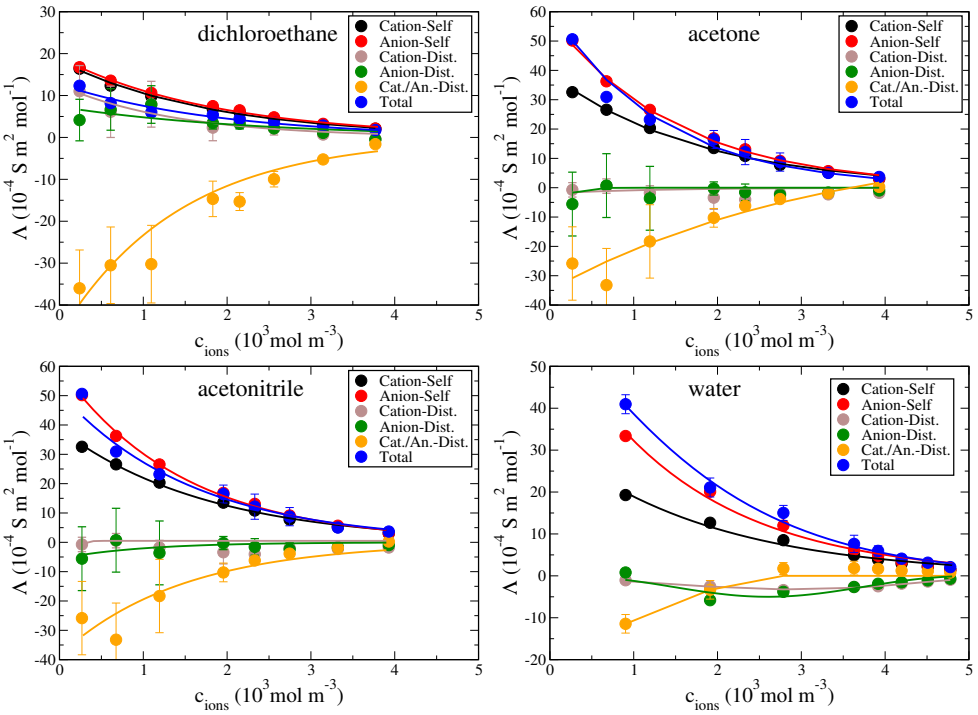

Figure 10: Self and distinct molar conductivities for $[BMIM^+][BF_4^-]$ / dichloroethane, acetone, acetonitrile, and water electrolytes at varying ion concentration (c_{ions}).

Peaks in the specific conductivities (Figure 9) are due to the multiplicative effect of increasing charge-carrier number and decreasing molar conductivity with increasing ion mole fraction; the molar conductivity is therefore much more monotonic, illustrating concentration-dependent trends. In Figure 10, we plot the molar conductivities of the electrolytes, for which the specific conductivities in Figure 9 are normalized by ion concentration. With the exception of the cation-distinct and anion-distinct conductivities in water, all self, distinct, and total molar conductivities exhibit largely monotonic concentration dependence. Molar conductivities for all the electrolytes are maximized at dilute concentrations, for which the ion self-diffusion is maximal due to the much lower viscosity of the solvents compared to the pure ionic liquid. While insightful, interpretation of concentration-dependent collective-ion phenomena is obscured by this very large viscosity effect. Greater insight is achieved by analyzing the fractional contribution of each conductivity term as a function of ion concentration; such a comparison in made in Figure 11.

In Figure 11, an important trend emerges indicating a shift in the nature of collective ion

motion from the dilute to concentrated electrolyte limit. We group the self conductivity terms ($\sigma^s_{cat} + \sigma^s_{an}$) and the like-ion distinct terms ($\sigma^d_{cat} + \sigma^d_{an}$), and compare the fractional contribution of these with the cation/anion-distinct conductivity ($\sigma^d_{cat,an}$) contribution. At low concentration, the primary collective ion motion consists of negative cation/anion-distinct contributions; the like-ion distinct terms are either small (no-correlation) or positive if the cation/anion-distinct correlation is sufficiently large (ion-pairing, dichloroethane). The interpretation is that ion motion is mostly independent and uncorrelated in the absence of ion-pairing, with ion-pairing effects important for lower dielectric solvents. The ion concentration is not high enough for like-ion correlation to be important in the absence of ion clustering; if ion clustering is present, it is indicated by a very large magnitude (negative) cation/anion-distinct conductivity term and positive like-ion distinct term (dichloroethane electrolytes). At higher-concentration, however, the collective-ion phenomena is very different. Anti-correlated, like-ion motion becomes increasingly important at higher concentration, and is the dominant correlation effect in the limit of the pure ionic liquid; this is indicated by the negative like-ion distinct conductivity for all electrolytes at sufficiently high ion concentration. The greater influence of anti-correlated, like-ion motion compared to counterion correlation on the pure ionic liquid collective motion has been previously noted,[36] and is similar to findings for molten alkali halide salts based on similar analysis.[74] For concentrated electrolytes at or above ~ 0.5 ion mole fraction, Figure 11 indicates that the collective ion motion becomes qualitatively similar to the behavior of the pure ionic liquid (χ=1), with the exception being the low-dielectric, dichloroethane electrolytes.

The analysis presented in Figure 11 provides a powerful framework for interpreting collective ion phenomena in organic electrolytes. Solvent dielectric strength and ion concentration effects are independently isolated from the order(s) of magnitude drop in ion diffusion rates due to the similarly large increasing viscosity. The influence of solvent dielectric strength is clearly illustrated by the magnitude of the cation/anion-distinct conductivity at low ion content for different electrolytes; this term is increasingly large and negative for lower dielectric

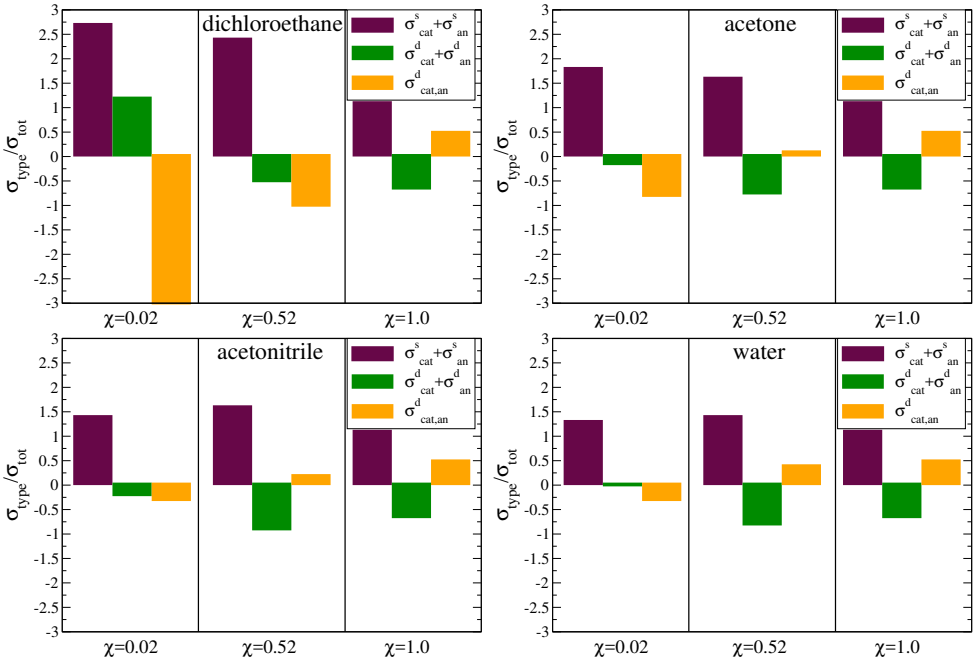

Figure 11: Fractional contribution of self and distinct conductivity terms at χ=0.02, χ=0.52, and χ=1.0 (neat ionic liquid) mole fraction of [BMIM$^+$][BF$_4^-$] ions in dichloroethane, acetone, acetonitrile, and water electrolytes. Plotted values are the ratio of the conductivity groups $\sigma^s_{cat} + \sigma^s_{an}$, $\sigma^d_{cat} + \sigma^d_{an}$, and $\sigma^d_{cat,an}$ to the total conductivity (σ_{tot}) at the specified concentration.

solvents, indicating substantial ion pairing. Comparing moderate dielectric (acetone) to low-dielectric (dichloroethane) electrolytes at χ=0.02, the reduction in dielectric screening results in significantly greater ion-pairing (larger, negative cation/anion-distinct contribution), leading to clustering, and positive, correlated like-ion motion (positive like-ion distinct terms). The other notable regime of collective ion dynamics is evident at higher concentrations, with the onset of larger, negative like-ion distinct conductivities. In this regime, like-ions are anti-correlated and diffuse in opposite directions as a consequence of local charge neutrality and screening requirements. For electrolytes composed of low to moderate dielectric solvents, increasing ion concentration alters the primary collective ion processes from being dominated by counterion correlation at low concentration, to dominated by like-ion, anti-correlation at moderate to high concentration, which is clearly shown in the analysis of the distinct conductivity terms for dichloroethane and acetone electrolytes in Figure 11. For the higher dielectric electrolytes (acetonitrile, water), the corresponding transition is from little to no ion correlation at low concentration, to a similar regime of like-ion anti-correlation at high ion concentration.

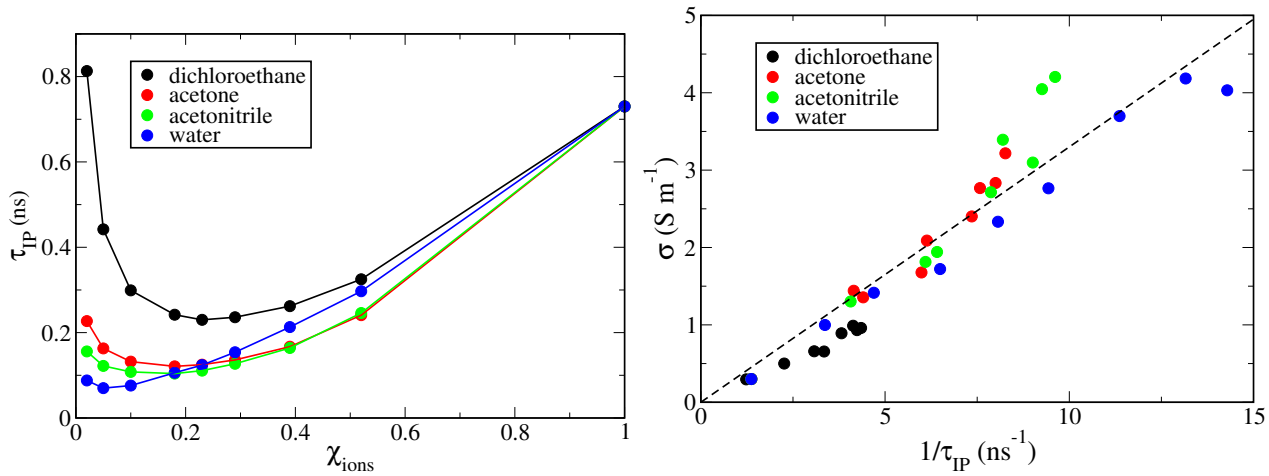

Figure 12: a) Ion pair lifetimes in $[BMIM^+][BF_4^-]$ / dichloroethane, acetone, acetonitrile, and water electrolytes at varying ion concentration (c_{ions}). b) Correlation between conductivity and inverse ion pair lifetime in the electrolytes. We note that the error bars shown in Figure 9 have been removed here for clarity.

Lastly, we examine the lifetimes of ion pairs within the electrolytes. Based on previous analysis of the ion diffusion coefficients and the self and distinct conductivities, it is expected that the ion pair lifetimes exhibit substantial concentration and solvent dependence. In Figure 12a, we show the ion pair lifetime as a function of concentration in the different electrolytes. The concentration dependence is non-monotonic, with lifetimes initially decreasing with concentration, passing through a minima, and then increasing again to the neat ionic liquid limit. As expected, for the dilute electrolytes, ion pair lifetimes increase with decreasing solvent dielectric strength. For the low dielectric, dichloroethane electrolytes, the lifetime of $[\mathrm{BMIM}^+][\mathrm{BF}_4^-]$ ion pairs is nearly ~ 1 ns at dilute concentrations, which is consistent with the large, negative $\sigma^d_{cat,an}$ conductivity values, and previously computed ion-association free energies.[57] The physical origin of the non-monotonic concentration dependence of the ion pair lifetimes is similar to that dictating the non-monotonic trends in the specific conductivities (Figure 9). For dilute electrolytes, the lifetime decreases with increasing concentration as there are more possible counterions to pair with. However, the viscosity of the electrolyte increases substantially with ion content, and this results in the minima and subsequent increase in ion pair lifetimes as the liquid dynamics are dramatically slowed while approaching the neat ionic liquid limit.

To illustrate that similar physics dictates the concentration-dependent trends in the ion pair lifetimes and specific conductivities, in Figure 12b we plot the conductivity vs inverse lifetime for all electrolytes. We find that there is good correlation between these quantities, with a slope of ~ 0.33 and $R^2 \sim 0.94$ for the linear regression. This finding is similar to previous conclusions of Zhang and Maginn, who observed good correlation between inverse ion pair lifetimes and the ion diffusion coefficients and Nernst-Einstein conductivities of 29 different ionic liquids.[70] It is remarkable to us that such a correlation is maintained for the diverse electrolytes studied in this work, which encompass a range of concentrations and solvent dielectric strength. The conclusion of Zhang and Maginn, that "transport properties of ionic liquids are governed by a universal mechanism related to the rate with which coun-

terions exit and leave their local coordination environment",[70] seems to be more generally applicable to organic electrolytes of all concentrations. We note that a similar regression for inverse lifetime and Nernst-Einstein conductivity (σ_{tot}^{NE}) for the electrolytes considered in this work exhibits significantly lower correlation ($R^2 \sim 0.86$), verifying that collective dynamics modulates ion association processes at all concentrations, especially for electrolytes comprised of lower-dielectric solvents.

4 Conclusion

In any ionic media, strong Coulomb interactions result in ionic correlation due to attraction of counterions and repulsion of like ions; however as we have shown in this work, such correlation is particularly important when there is low-dielectric solvent. In this regard, organic electrolytes differ from aqueous electrolytes in the relative importance of ion correlation and collective ion processes. The extent of ion correlation significantly increases going from water, to acetonitrile, to acetone, to dichloroethane-based electrolytes, due to reduced dielectric screening. In fact, for dichloroethane-based electrolytes, we have shown that it is inappropriate to think of isolated ions, but rather ions predominently exist as ion pairs or clusters, even at very dilute concentrations!

We have illustrated both structural and dynamical signatures of changing ion correlation from the dilute electrolyte to the pure ionic liquid limit. Cation-anion ion-pair coordination motifs are qualitatively similar at all concentrations, evidenced by similar-distance peaks in the pairwise probability distributions; however the extent of ion pairing and coordination number at dilute conditions depends sensitively on solvent dielectric strength. Also interesting is the onset of secondary ion structure, or ion layering with increasing concentration. This is evidenced by secondary peaks in the cation/anion distribution, and primary peaks in the like-ion, cation/cation and anion/anion distributions. Low dielectric solvents promote ion clustering, resulting in the onset of ion secondary structure at lower

ion concentrations. Corresponding signatures are observed in the dynamic properties of the electrolytes. Clustering and onset of ion secondary structure in dichloroethane solvents is evidenced by both the quantitative similarity of cation and anion diffusion coefficients, and large negative cation/anion-distinct and positive like-ion-distinct fractional conductivities. For concentrated electrolytes, the formation of ion secondary structure results in significant anti-correlated like-ion motion, indicated by the negative like-ion distinct conductivity contributions. We propose that analysis of the fractional contribution of self and distinct conductivity terms (Figure 11) provides a clear illustration of the transition of collective ion phenomena spanning the dilute to pure ionic liquid limit.

Through systematic analysis of the full concentration range, we conclude that the behavior of dilute electrolytes is very different from concentrated electrolytes and pure ionic liquids based on their qualitatively distinct collective ion dynamics.[41] In the dilute limit, any significant collective process is mediated by counterion attraction (negative cation/anion-distinct conductivities), while in concentrated electrolytes the dominant influence is anti-correlated, like-ion motion giving rise to negative like-ion-distinct conductivities. Despite this important difference, we find good correlation between the inverse ion-pair lifetimes and specific conductivities for all electrolytes of different concentration and different solvent dielectric strength. This remarkable extension of the conclusions of Zhang and Maginn[70] for pure ionic liquids suggests that formation and dissolution of ion pairs is a fundamental mechanism dictating electrolyte conductivity in all systems.

What are the consequences for electrochemical applications of these electrolytes? The extent of ion pairing is an extremely important property of the electrolyte in this regard. For example, energy storage in electrical double layer supercapacitors depends on energy differences between ions in the bulk and at electrode interfaces; low-dielectric solvents (dichloroethane) may thus provide higher energy systems due to the prevalent ion pairing in the bulk.[18] Consequently, however, conductivities of these electrolytes are relatively low, due to large, negative cation/anion distinct contributions, caused by ion pairing. Mixtures may be utilized

for intelligently designed, simultaneous property optimization, leading to even more complex and correlated physical processes. Due to the dramatic property variation with solvent dielectric strength and ion concentration, there is much room for tuning organic electrolytes for optimal performance in their numerous applications.

5 Acknowledgments

This research was supported in part through research cyberinfrastructure resources and services provided by the Partnership for an Advanced Computing Environment (PACE) at the Georgia Institute of Technology, Atlanta, Georgia, USA.

References

(1) Zhang, S. S. A Review on Electrolyte Additives for Lithium-Ion Batteries. *J. Power Sources* **2006**, *162*, 1379–1394.

(2) Fedorov, M. V.; Kornyshev, A. A. Ionic Liquids at Electrified Interfaces. *Chem. Rev.* **2014**, *114*, 2978–3036.

(3) Cheng, L.; Assary, R. S.; Qu, X.; Jain, A.; Ong, S. P.; Rajput, N. N.; Persson, K.; Curtiss, L. A. Accelerating Electrolyte Discovery for Energy Storage with High-Throughput Screening. *J. Phys. Chem. Lett.* **2015**, *6*, 283–291.

(4) Miller, J. R.; Simon, P. Electrochemical Capacitors for Energy Management. *Science* **2008**, *321*, 651–652.

(5) VanAken, K. L.; Beidaghi, M.; Gogotsi, Y. Formulation of Ionic-Liquid Electrolyte To Expand the Voltage Window of Supercapacitors. *Angew. Chem. Int. Ed.* **2015**, *54*, 4806–4809.

(6) Armand, M.; Endres, F.; MacFarlane, D. R.; Ohno, H.; Scrosati, B. Ionic-liquid Materials for the Electrochemical Challenges of the Future. *Nat Mater* **2009**, *8*, 621–629, 10.1038/nmat2448.

(7) Maginn, E. J. Molecular Simulation of Ionic Liquids: Current Status and Future Opportunities. *J. Phys. Condens. Matter* **2009**, *21*, 373101.

(8) Castner, E. W.; Wishart, J. F. Spotlight on Ionic Liquids. *J. Chem. Phys.* **2010**, *132*, 120901.

(9) Dommert, F.; Wendler, K.; Berger, R.; Delle Site, L.; Holm, C. Force Fields for Studying the Structure and Dynamics of Ionic Liquids: A Critical Review of Recent Developments. *ChemPhysChem* **2012**, *13*, 1625–1637.

(10) Salanne, M. Simulations of Room Temperature Ionic Liquids: from Polarizable to Coarse-Grained Force Fields. *Phys. Chem. Chem. Phys.* **2015**, *17*, 14270–14279.

(11) Nishida, T.; Tashiro, Y.; Yamamoto, M. Physical and Electrochemical Properties of 1-alkyl-3-methylimidazolium Tetrafluoroborate for Electrolyte. *J. Fluorine Chem.* **2003**, *120*, 135–141.

(12) Stoppa, A.; Hunger, J.; Buchner, R. Conductivities of Binary Mixtures of Ionic Liquids with Polar Solvents. *J. Chem. Eng. Data* **2009**, *54*, 472–479.

(13) Stoppa, A.; Zech, O.; Kunz, W.; Buchner, R. The Conductivity of Imidazolium-Based Ionic Liquids from (35 to 195) C. A. Variation of Cations Alkyl Chain. *J. Chem. Eng. Data* **2010**, *55*, 1768–1773.

(14) Canongia Lopes, J. N.; Costa Gomes, M. F.; Husson, P.; Padua, A. A. H.; Rebelo, L. P. N.; Sarraute, S.; Tariq, M. Polarity, Viscosity, and Ionic Conductivity of Liquid Mixtures Containing [C4C1im][Ntf2] and a Molecular Component. *J. Phys. Chem. B* **2011**, *115*, 6088–6099.

(15) Kalugin, O. N.; Voroshylova, I. V.; Riabchunova, A. V.; Lukinova, E. V.; Chaban, V. V. Conductometric Study of Binary Systems Based on Ionic Liquids and Acetonitrile in a Wide Concentration Range. *Electrochimica Acta* **2013**, *105*, 188–199.

(16) Stassen, H. K.; Ludwig, R.; Wulf, A.; Dupont, J. Imidazolium Salt Ion Pairs in Solution. *Chem. Eur. J.* **2015**, *21*, 8324–8335.

(17) Li, W.; Zhang, Z.; Han, B.; Hu, S.; Xie, Y.; Yang, G. Effect of Water and Organic Solvents on the Ionic Dissociation of Ionic Liquids. *J. Phys. Chem. B* **2007**, *111*, 6452–6456.

(18) Bozym, D. J.; Uralcan, B.; Limmer, D. T.; Pope, M. A.; Szamreta, N. J.; Debenedetti, P. G.; Aksay, I. A. Anomalous Capacitance Maximum of the Glassy Carbon-Ionic Liquid Interface through Dilution with Organic Solvents. *J. Phys. Chem. Lett.* **2015**, *6*, 2644–2648.

(19) Uralcan, B.; Aksay, I. A.; Debenedetti, P. G.; Limmer, D. T. Concentration Fluctuations and Capacitive Response in Dense Ionic Solutions. *J. Phys. Chem. Lett.* **2016**, *7*, 2333–2338.

(20) Asaki, M. L. T.; Redondo, A.; Zawodzinski, T. A.; Taylor, A. J. Dielectric Relaxation and Underlying Dynamics of Acetonitrile and 1-Ethyl-3-methylimidazolium Triflate Mixtures Using THz Transmission Spectroscopy. *J. Chem. Phys.* **2002**, *116*, 10377–10385.

(21) Asaki, M. L. T.; Redondo, A.; Zawodzinski, T. A.; Taylor, A. J. Dielectric Relaxation of Electrolyte Solutions Using Terahertz Transmission Spectroscopy. *J. Chem. Phys.* **2002**, *116*, 8469–8482.

(22) Wakai, C.; Oleinikova, A.; Ott, M.; Weingrtner, H. How Polar Are Ionic Liquids? Determination of the Static Dielectric Constant of an Imidazolium-based Ionic Liquid by Microwave Dielectric Spectroscopy. *J. Phys. Chem. B* **2005**, *109*, 17028–17030.

(23) Hunger, J.; Stoppa, A.; Buchner, R.; Hefter, G. From Ionic Liquid to Electrolyte Solution: Dynamics of 1-N-Butyl-3-N-methylimidazolium Tetrafluoroborate/Dichloromethane Mixtures. *J. Phys. Chem. B* **2008**, *112*, 12913–12919.

(24) Hunger, J.; Stoppa, A.; Schrdle, S.; Hefter, G.; Buchner, R. Temperature Dependence of the Dielectric Properties and Dynamics of Ionic Liquids. *ChemPhysChem* **2009**, *10*, 723–733.

(25) Nakamura, K.; Shikata, T. Systematic Dielectric and NMR Study of the Ionic Liquid 1-Alkyl-3-Methyl Imidazolium. *ChemPhysChem* **2010**, *11*, 285–294.

(26) Turton, D. A.; Hunger, J.; Hefter, G.; Buchner, R.; Wynne, K. Glasslike Behavior in Aqueous Electrolyte Solutions. *J. Chem. Phys.* **2008**, *128*, 161102.

(27) Turton, D. A.; Hunger, J.; Stoppa, A.; Hefter, G.; Thoman, A.; Walther, M.; Buchner, R.; Wynne, K. Dynamics of Imidazolium Ionic Liquids from a Combined Dielectric Relaxation and Optical Kerr Effect Study: Evidence for Mesoscopic Aggregation. *J. Am. Chem. Soc.* **2009**, *131*, 11140–11146.

(28) Buchner, R.; Hefter, G. Interactions and Dynamics in Electrolyte Solutions by Dielectric Spectroscopy. *Phys. Chem. Chem. Phys.* **2009**, *11*, 8984–8999.

(29) Caillol, J. M.; Levesque, D.; Weis, J. J. Electrical Properties of Polarizable Ionic Solutions. II. Computer Simulation Results. *J. Chem. Phys.* **1989**, *91*, 5555–5566.

(30) Schroder, C.; Wakai, C.; Weingrtner, H.; Steinhauser, O. Collective Rotational Dynamics in Ionic Liquids: A Computational and Experimental Study of 1-butyl-3-methylimidazolium Tetrafluoroborate. *J. Chem. Phys.* **2007**, *126*, 084511.

(31) Schroder, C.; Haberler, M.; Steinhauser, O. On the Computation and Contribution of Conductivity in Molecular Ionic Liquids. *J. Chem. Phys.* **2008**, *128*, 134501.

(32) Schroder, C.; Sonnleitner, T.; Buchner, R.; Steinhauser, O. The Influence of Polarizability on the Dielectric Spectrum of the Ionic Liquid 1-Ethyl-3-methylimidazolium Triflate. *Phys. Chem. Chem. Phys.* **2011**, *13*, 12240–12248.

(33) Tokuda, H.; Hayamizu, K.; Ishii, K.; Susan, M. A. B. H.; Watanabe, M. Physicochemical Properties and Structures of Room Temperature Ionic Liquids. 1. Variation of Anionic Species. *J. Phys. Chem. B* **2004**, *108*, 16593–16600.

(34) Tokuda, H.; Hayamizu, K.; Ishii, K.; Susan, M. A. B. H.; Watanabe, M. Physicochemical Properties and Structures of Room Temperature Ionic Liquids. 2. Variation of Alkyl Chain Length in Imidazolium Cation. *J. Phys. Chem. B* **2005**, *109*, 6103–6110.

(35) Tokuda, H.; Tsuzuki, S.; Susan, M. A. B. H.; Hayamizu, K.; Watanabe, M. How Ionic Are Room-Temperature Ionic Liquids? An Indicator of the Physicochemical Properties. *J. Phys. Chem. B* **2006**, *110*, 19593–19600.

(36) Harris, K. R. Can the Transport Properties of Molten Salts and Ionic Liquids Be Used To Determine Ion Association? *J. Phys. Chem. B* **2016**, *120*, 12135–12147.

(37) Raineri, F. O.; Friedman, H. L. Velocity Correlations in the Molecular Dynamics Ensemble: Computation of the Distinct Diffusion Coefficients. *J. Chem. Phys.* **1989**, *91*, 5642–5647.

(38) Padro, J. A.; Trullas, J.; Sese, G. Computer Simulation Study of the Dynamic Cross-Correlations in Liquids. *Mol. Phys.* **1991**, *72*, 1035–1049.

(39) Kashyap, H. K.; Annapureddy, H. V. R.; Raineri, F. O.; Margulis, C. J. How Is Charge Transport Different in Ionic Liquids and Electrolyte Solutions? *J. Phys. Chem. B* **2011**, *115*, 13212–13221.

(40) Eilmes, A.; Kubisiak, P. Quantum-Chemical and Molecular Dynamics Study of M+[TOTO]-(M = Li, Na, K) Ionic Liquids. *J. Phys. Chem. B* **2013**, *117*, 12583–12592.

(41) Lee, A. A.; Vella, D.; Perkin, S.; Goriely, A. Are Room-Temperature Ionic Liquids Dilute Electrolytes? *J. Phys. Chem. Lett.* **2015**, *6*, 159–163.

(42) Wu, X.; Liu, Z.; Huang, S.; Wang, W. Molecular Dynamics Simulation of Room-temperature Ionic Liquid Mixture of [bmim][BF4] and Acetonitrile by a Refined Force Field. *Phys. Chem. Chem. Phys.* **2005**, *7*, 2771–2779.

(43) Chaban, V. V.; Prezhdo, O. V. A New Force Field Model of 1-Butyl-3-methylimidazolium Tetrafluoroborate Ionic Liquid and Acetonitrile Mixtures. *Phys. Chem. Chem. Phys.* **2011**, *13*, 19345–19354.

(44) Jenel, V.; Mihaela, V.; Oleg, B.; Dmitry, B. A Comparative Study of Room Temperature Ionic Liquids and Their Organic Solvent Mixtures Near Charged Electrodes. *J. Phys. Condens. Matter* **2016**, *28*, 464002.

(45) Lee, B.-S.; Lin, S.-T. A Priori Prediction of Dissociation Phenomena and Phase Behaviors of Ionic Liquids. *Ind. Eng. Chem. Res.* **2015**, *54*, 9005–9012.

(46) Osti, N. C.; Van Aken, K. L.; Thompson, M. W.; Tiet, F.; Jiang, D.-e.; Cummings, P. T.; Gogotsi, Y.; Mamontov, E. Solvent Polarity Governs Ion Interactions and Transport in a Solvated Room-Temperature Ionic Liquid. *J. Phys. Chem. Lett.* **2017**, *8*, 167–171.

(47) Schroder, C.; Rudas, T.; Neumayr, G.; Benkner, S.; Steinhauser, O. On the Collective Network of Ionic Liquid/Water Mixtures. I. Orientational Structure. *J. Chem. Phys.* **2007**, *127*, 234503.

(48) Schroder, C.; Neumayr, G.; Steinhauser, O. On the Collective Network of Ionic Liquid/Water Mixtures. III. Structural Analysis of Ionic Liquids on the Basis of Voronoi Decomposition. *J. Chem. Phys.* **2009**, *130*, 194503.

(49) Schroder, C.; Sega, M.; Schmollngruber, M.; Gailberger, E.; Braun, D.; Steinhauser, O. On the Collective Network of Ionic Liquid/Water Mixtures. IV. Kinetic and Rotational Depolarization. *J. Chem. Phys.* **2014**, *140*, 204505.

(50) Sieffert, N.; Wipff, G. The [BMI][Tf2N] Ionic Liquid/Water Binary System: A Molecular Dynamics Study of Phase Separation and of the Liquid-Liquid Interface. *J. Phys. Chem. B* **2006**, *110*, 13076–13085.

(51) Rollet, A.-L.; Porion, P.; Vaultier, M.; Billard, I.; Deschamps, M.; Bessada, C.; Jouvensal, L. Anomalous Diffusion of Water in [BMIM][TFSI] Room-Temperature Ionic Liquid. *J. Phys. Chem. B* **2007**, *111*, 11888–11891.

(52) Kelkar, M. S.; Shi, W.; Maginn, E. J. Determining the Accuracy of Classical Force Fields for Ionic Liquids: Atomistic Simulation of the Thermodynamic and Transport Properties of 1-Ethyl-3-methylimidazolium Ethylsulfate ([emim][EtSO4]) and Its Mixtures with Water. *Ind. Eng. Chem. Res.* **2008**, *47*, 9115–9126.

(53) Umebayashi, Y.; Jiang, J.-C.; Shan, Y.-L.; Lin, K.-H.; Fujii, K.; Seki, S.; Ishiguro, S.-I.; Lin, S. H.; Chang, H.-C. Structural Change of Ionic Association in Ionic Liquid/Water Mixtures: A High-pressure Infrared Spectroscopic Study. *J. Chem. Phys.* **2009**, *130*, 124503.

(54) Yee, P.; Shah, J. K.; Maginn, E. J. State of Hydrophobic and Hydrophilic Ionic Liquids in Aqueous Solutions: Are the Ions Fully Dissociated? *J. Phys. Chem. B* **2013**, *117*, 12556–12566.

(55) Sha, M.; Dong, H.; Luo, F.; Tang, Z.; Zhu, G.; Wu, G. Dilute or Concentrated Electrolyte Solutions? Insight from Ionic Liquid/Water Electrolytes. *J. Phys. Chem. Lett.* **2015**, *6*, 3713–3720.

(56) Borodin, O.; Price, D. L.; Aoun, B.; Gonzalez, M. A.; Hooper, J. B.; Kofu, M.; Ko-

hara, S.; Yamamuro, O.; Saboungi, M.-L. Effect of Water on the Structure of a Prototype Ionic Liquid. *Phys. Chem. Chem. Phys.* **2016**, *18*, 23474–23481.

(57) McDaniel, J. G. Polarization Effects in Binary [BMIM+][BF4-]/1,2-Dichloroethane, Acetone, Acetonitrile, and Water Electrolytes. *J. Phys. Chem. B* **2018**, *122*, 4345–4355.

(58) Borodin, O. Polarizable Force Field Development and Molecular Dynamics Simulations of Ionic Liquids. *J. Phys. Chem. B* **2009**, *113*, 11463–11478.

(59) Bedrov, D.; Borodin, O.; Li, Z.; Smith, G. D. Influence of Polarization on Structural, Thermodynamic, and Dynamic Properties of Ionic Liquids Obtained from Molecular Dynamics Simulations. *J. Phys. Chem. B* **2010**, *114*, 4984–4997.

(60) Choi, E.; McDaniel, J. G.; Schmidt, J. R.; Yethiraj, A. First-Principles, Physically Motivated Force Field for the Ionic Liquid [BMIM][BF4]. *J. Phys. Chem. Lett.* **2014**, *5*, 2670–2674.

(61) McDaniel, J. G.; Choi, E.; Son, C. Y.; Schmidt, J. R.; Yethiraj, A. Ab Initio Force Fields for Imidazolium-Based Ionic Liquids. *J. Phys. Chem. B* **2016**, *120*, 7024–7036.

(62) McDaniel, J. G.; Schmidt, J. R. First-Principles Many-Body Force Fields from the Gas Phase to Liquid: A "Universal" Approach. *J. Phys. Chem. B* **2014**, *118*, 8042–8053.

(63) Lamoureux, G.; Harder, E.; Vorobyov, I. V.; Roux, B.; MacKerell Jr, A. D. A Polarizable Model of Water for Molecular Dynamics Simulations of Biomolecules. *Chem. Phys. Lett.* **2006**, *418*, 245–249.

(64) Eastman, P.; Friedrichs, M. S.; Chodera, J. D.; Radmer, R. J.; Bruns, C. M.; Ku, J. P.; Beauchamp, K. A.; Lane, T. J.; Wang, L.-P.; Shukla, D. et al. OpenMM 4: A Reusable, Extensible, Hardware Independent Library for High Performance Molecular Simulation. *J. Chem. Theory Comput.* **2013**, *9*, 461–469.

(65) Lamoureux, G.; Roux, B. Modeling Induced Polarization with Classical Drude Oscillators: Theory and Molecular Dynamics Simulation Algorithm. *J. Chem. Phys.* **2003**, *119*, 3025–3039.

(66) Basconi, J. E.; Shirts, M. R. Effects of Temperature Control Algorithms on Transport Properties and Kinetics in Molecular Dynamics Simulations. *J. Chem. Theory Comput.* **2013**, *9*, 2887–2899.

(67) Essmann, U.; Perera, L.; Berkowitz, M. L.; Darden, T.; Lee, H.; Pedersen, L. G. A Smooth Particle Mesh Ewald Method. *J. Chem. Phys.* **1995**, *103*, 8577–8593.

(68) Martinez, L.; Andrade, R.; Birgin, E. G.; Martinez, J. M. PACKMOL: A Package for Building Initial Configurations for Molecular Dynamics Simulations. *J. Comput. Chem.* **2009**, *30*, 2157–2164.

(69) Chandler, D. *Introduction to Modern Statistical Mechanics*; Oxford University Press, 1987.

(70) Zhang, Y.; Maginn, E. J. Direct Correlation between Ionic Liquid Transport Properties and Ion Pair Lifetimes: A Molecular Dynamics Study. *J. Phys. Chem. Lett.* **2015**, *6*, 700–705.

(71) Borodin, O.; Smith, G. D. Development of Many-Body Polarizable Force Fields for Li-Battery Applications: 2. LiTFSI-Doped Oligoether, Polyether, and Carbonate-Based Electrolytes. *J. Phys. Chem. B* **2006**, *110*, 6293–6299.

(72) Son, C. Y.; McDaniel, J. G.; Schmidt, J. R.; Cui, Q.; Yethiraj, A. First Principles United Atom Force Field for the Ionic Liquid [BMIM][BF4] : An Alternative to Charge Scaling. *J. Phys. Chem. B* **2016**, *120*, 3560–3568.

(73) Casteel, J. F.; Amis, E. S. Specific Conductance of Concentrated Solutions of Magnesium Salts in Water-ethanol System. *J. Chem. Eng. Data* **1972**, *17*, 55–59.

(74) Trullas, J.; Padro, J. A. Diffusive Transport Properties in Monovalent and Divalent Metal-ion Halide Melts: A Computer Simulation Study. *Phys. Rev. B* **1997**, *55*, 12210–12217.

Graphical TOC Entry